CORRELATION TRACKING FOR A PLANETARY POINTING AND TRACKING SYSTEM

Touraj Assefi
The author is at the Jet Propulsion Laboratory,
California Institute of Technology,
Pasadena, California

ABSTRACT

The Planetary Pointing and Tracking System (PPTS) being developed at Jet Propulsion Laboratory is intended to provide precision pointing for science platforms on future autonomous planetary spacecraft. Future missions will impose very stringent platform pointing requirements due to low light levels and very high ground tracking rates. An integral part of PPTS is the correlation tracker, which has the potential to revolutionize autonomous guidance. The tracker provides two-axis pointing information concerning the position of the target body. It consists of a large-area charge-coupled device (CCD) imager and a microprocessor to control the CCD scanning function and data processing. The correlation tracker has three modes of operation: track, acquire and map. The track mode performs precision tracking of a target object. This is initiated after a target has been acquired. The map mode determes the centroidal coordinates, magnitude and size of bodies within the optical field of view. To improve precision pointing, various power spectra, such as shot noise and dark current, are derived. The probability of acquiring a target body is a function of signal-to-noise ratio and the noise equivalent angle. Derivations illustrating the application of these concepts are given. A discussion of mission analysis with the Uranian system as a representative example is provided.

Introduction

With flight times to the outer planets measured in years, and given the desire of the scientists to have the results of one mission influence the design of its successor, 1978 is by no means too early to be thinking of outer-planet programs which will last to the end of the century.

The missions will include orbiters, fly-bys, atmospheric probes, etc. The majority of planetary orbiters must include multiple satellite encounters among their objectives. For example, a Jupiter or Titan-Saturn fly-by with a Uranus orbiter combination might be extremely valuable.

With the use of advanced on-board system such as charge-coupled devices (CCDs) for imaging and data storage, vast amounts of high-quality data from the outer planets can be returned to Earth. Therefore, the use of advanced onboard imaging systems requires an equally advanced science platform articulation capability for any missions beyond 10 AU (Astronomical Unit).

JPL has taken the initiative in building the Planetary Pointing and Tracking Systems (PPTS) which is intended to provide precision pointing of the science platform on future unmanned planetary spacecraft. Because such missions will have very stringent platform pointing accuracy and stability requirements due to low light levels and very high ground tracking rates, present pointing capabilities will become inadequate. For example, the pointing accuracy of the Voyager scan platform is 0.14° (without the inclusion of trajectory errors) and the pointing requirement for the Galileo mission is of the same order, while the PPTS requirement is 10 $\widehat{\text{sec}}$. The tracker along with a gyro will decouple the platform from spacecraft motions.

Some of the most important new features and capabilities of the PPTS are:

a. Multispectral imaging to allow determination of planetary constituents, spatial distributions, and motions as well as their physical properties and structures.
b. Determination of surface features of the candidate planet and its satellites with very high resolution.
c. Reduction in the total number of mission images required, allowing for increased sequence time needed for completing science experiments as well as lower processing cost.
d. Exploration of the interplanetary and inter-stellar media to and beyond 20 AU with special emphasis on the region beyond Jupiter and Saturn. An example to satisfy the low light level requirement would be an exploration of the Uranian system with a Jupiter or Saturn fly-by.

The correlation tracker is a derivative of the STELLAR (Star Tracker for Economical Long Life Attitude Reference) developed at JPL [1]. The tracker consists of an area-imager charged coupled device (CCD) placed at the optical focus and a microprocessor to control the CCD scanning functions and data processing. The CCD integrates a charged pattern corresponding to a feature or landmark imaged upon it during the integration time. The charge pattern is then serially read out to an analog-to-digital converter. The image sensor is a Fairchild 221 CCD (488 x 380 pixels). The correlation tracker has three mode of operation: track, acquire, and map. The track mode performs precision tracking of a target body. This is initiated after a target body has been acquired. The map mode determines centroidal coordinates, magnitude and size of bodies within the optical field of view. It is well known [2] that the probability of correct target acquisition is a function of

signal-to-noise ratio (SNR), which to avoid a false lock, should be as high as possible. The noise sources in the correlation tracker must be identified before we can derive the signal-to-noise ratio. However, it must be emphasized that noise is not the only source of errors. In general the accuracy of the correlation tracker will be affected by several error sources, some of which are removable or reducible by calibration. We shall not address the removable error sources in this paper.

CCD Noise Sources and Their Statistics

Since the probability of acquisition is a function of signal-to-noise ratio, it is necessary to analyze the noise sources in the CCD. The noise sources in the CCD occur in four categories. They are (1) transfer loss noise, (2) background charged generation noise, (3) output amplifier noise, and (4) fast interface state trapping noise. A schematic diagram of CCD noise sources if given via Fig. 1. In what follows a discussion of each category will be given, with the noise sources characterized by their standard deviations.

1. Transfer Loss Noise

In an ideal system, the charge measured in the output and attributable to a given light-sensitive element would be directly related to the integrated light intensity incident on the light-sensitive element. In reality, however, if N_s is the total number of carriers in the signal packet, a fraction ϵ of the charge N_s will fail to be transferred each time, which implies that on the average ϵN_s will be lost. Thus the fluctuations about the average will be $2 \epsilon N_s$ due to the entry and exit at the potential well. The transfer efficiency can be as high as 99. 99% which implies that the effect of this noise will be extremely small.

2. Background Charge Generation Noise

Background noise may be generated at the input electrically, optically, or thermally.

The noise is attributed to any of the following sources:

(a) Photon noise: Experimental evidence shows that the emission of photons from a given source is a Poisson random process. Thus the number of photoelectrons collected in a potential well in time τ is a Poisson process with its standard deviation equal to the square root of the mean.

(b) Fat zero noise: The injection of charge from a diffusion source into a potential well is a stochastic process because of the nature of thermal noise associated with the input resistance. Hence an electrical input noise is generated due to the injection of electrons from the diffusion source into the potential well.

3. Output Amplifier Noise

   (a) Reset Noise: In most CCD devices, the readout process will cause the charging of a capacitance through a switch. This operation is called reset. The noise in the reset process is thermal and it is directly reflected in the output signal.

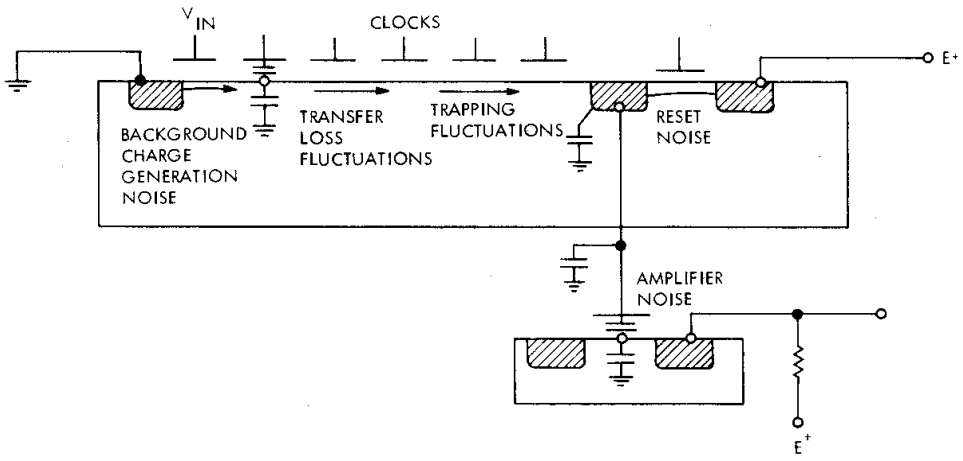

Fig. 1 — CCD with Various Noise Sources

   (b) Metal-Oxide-Semiconductor Field-Effect-Transistor Noise (MOSFET): This noise exists due to various noise sources in an MOS amplifier. Thus, the output voltage is a random process. Comparing this noise with the input as a charge on the gate, we can treat it like other noise sources.

4. Integration and Transfer Noise Sources:

   (a) The transfer of electrons from one place to another is a random process because of trapping and emission by fast and slow interface states as well as bulk states. Among the transfer noise sources, the semiconductor bulk trapping noise is a nonlinear function of the charge being transferred. However, it is shown that this error source is not dominant. A model for the bulk trapping noise is given in reference [3].

   (b) Dark Current Noise: It is well known that thermal generation of hole-electron pairs in semiconductors is a random process. Thus, it contributes charge (noise) to the CCD potential wells. This noise source process is a Poisson process.

As already mentioned, there are other sources of error which can be considered to be noise. Among them are: CCD pixel variable response, digital quantization errors, CCD pattern dimension errors, and signal process errors. We shall next discuss the statistics of the most representative noise sources in terms of their first two moments.

Thermal Noise Statistics

Several noise sources associated with CCD involve thermal or Johnson noise [1] of a resistance in parallel with a capacitor. The root-mean-square (rms) fluctuations in the number of carriers on the capacitor is desired, (see the diagram below). We know the average energy stored due to the resistor alone is 1/2 C v^2 which is equated with the thermodynamic energy of

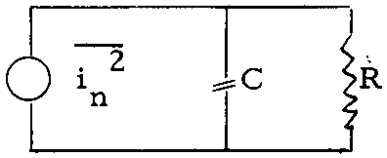

the system, i. e. , 1/2 kT, from which we can obtain

$$\overline{V^2} = \frac{kT}{C} \tag{1}$$

Thus the rms carrier fluctuation is

$$N = \frac{1}{q} C \overline{V} = \frac{1}{q} (kTC)^{1/2} = 400(C_{Pf})^{1/2} \tag{2}$$

Dark Current Shot Noise Statistics

As already mentioned the dark current electronic emission is time independent and obeys Poisson statistics. Thus the probability that m electrons are emitted in time τ is given by:

$$P[x(\tau) = m] = \frac{(\lambda\tau)^m \exp(-\lambda\tau)}{m!} \tag{3}$$

Where $x(\tau)$ is the stochastic process which equals the number of electrons in the interval $(0,\tau)$ and $\lambda = I_D/q$. Thus $\lambda\tau$ is the average number of dark current electrons released. Since the m electrons that are emitted in the interval $(0,\tau)$ each carry a unit electronic charge q, the total current is given by:

$$i_D(t) = \sum_{n=1}^{m} G\ q\ \delta(t-t_n) \tag{4}$$

where $-\tau/2 \le t \le \tau/2$, and $\delta(t-t_n)$ is the unit impulse function occuring at time τ_n and G is the gain of the detector.

It can be shown [4] that the autocorrelation function in terms of average number of dark current electrons is given by:

$$R(\gamma) = G^2 \, q \, I_D \, \delta(\lambda) + G^2 \, I_D^2 \tag{5}$$

The corresponding power spectrum is the Fourier transform of R, i.e.

$$S(w) = G^2 \, q \, I_D + 2\pi \, I_D^2 \, \delta(w) \tag{6}$$

However, the power spectrum passes through a band-pass filter, so the delta function in the power spectrum will drop out. It is well known [5] that a Poisson process x(t) will have the first two moments given by:

$$E\,x(t) = \lambda t \tag{7}$$

and

$$R_x(t_1, t_2) = E[x(t_1)\,x(t_2)] = \begin{cases} \lambda t_2 + \lambda^2 t_1 t_2 & t_1 \geq t_2 \\ \lambda t_1 + \lambda^2 t_1 t_2 & t_1 \leq t_2 \end{cases} \tag{8}$$

Thus the standard deviation σ_x is given by:

$$\sigma_x = [Ex^2(t) - E^2x(t)]^{1/2} = (\lambda t)^{1/2} \tag{9}$$

Approximate Numerical Values of Noise Sources

To obtain closed form solution for the noise equivalent signal (NES) the joint probability density function of the noise sources is required. This is impossible to obtain, although a Monte Carlo simulation can be used to obtain a very realistic numerical solution. However, we can obtain a more limited closed form result by introducing some simplifying approximations. While this approach is not optimal, it will nevertheless yield some revealing results.

The correlation tracker presently being developed at JPL utilizes a CCD, where there is a difference in the step size in the horizontal direction (denoted by j) and the vertical direction (denoted by k). The step sizes in the j-direction are twice as great as in the k-direction. To obtain uniformity in the two directions every other line of data in the k-direction is ignored. The purpose of the tracker is to select a small subset of pixels with high contrast areas to be processed in 0.1 s (or a maximum of 1 s). However, the noise sources must be considered for all pixels. Presently, the algorithm makes use of relative positions only and has no center finding capability. This is a reasonable approach, since for

an extended body or a landmark, the center of brightness may be very difficult to define. However, if a phypthetical center of brightness existed, every pixel in the CCD could be compared with it. Having made this assumption, and selecting a center finding algorithm given in references [1] and [6], the calculation of NES can be obtained analytically. It is reasonable to assume that 90% of the energy falls within 1.5 and 3 pixels in the horizontal and vertical directions, respectively. In reference [1] a 4 x 4 interpolation matrix is used which is a simplification of the centroid equation given by

$$x_c = \frac{\sum s_i x_i}{\sum s_i} \tag{10}$$

where s_i is the illuminance in a resolution element located a distance x_i from the coordinate reference. Let us apply the algorithm to the shot noise when we observe a point source. The signal collected by a CCD from the image of the point source is given in reference [7] as:

$$Q_s = \frac{Aaf\tau}{q} \int R(\lambda)S(\lambda)d\lambda \tag{11}$$

where A denotes the lens area, a the active area ratio, f the optical system transmission, τ the integration time, R the CCD spectral response, and S the power spectral density. The centroid x_c can be found via the 4 x 4 interpolation matrix in references [1] and [6] as:

$$x_c = \frac{Q_{k+3} - Q_{k+1} - 2Q_k}{Q_s} + \frac{1}{2} \tag{12}$$

where the Q_k's are charge levels corresponding to the horizontal direction and having been summed in the vertical direction. Now it is desired to obtain the standard deviation of x_c, which we denote by σ_x, or n_s. It is obvious that Q_k and Q_s are random variables. The calculation of σ_x requires knowledge of the joint probability density function of every term involved in the right hand side of equation (12). This information is not available. However, since Q_s represents a large amount of charge (electrons), it can be assumed to be a deterministic quantity and the calculation of σ_x becomes very simple, thus:

$$\sigma_x = n_s = \frac{[\sigma_{k+3}^2 + \sigma_{k+1}^2 + (2\sigma_k)^2]^{1/2}}{Q_s} \tag{13}$$

Now making use of the fact that electrons hitting the detector are Poisson distributed and the standard deviation of the Poisson process equals the square root of its mean, a further simplification can result:

$$\sigma_x \approx 0.91 (Q_s)^{-\frac{1}{2}} \tag{14}$$

Now, if we look at the target from a long distance and substitute from equation (11) with the corresponding parameters given in re ference [7], we find:

$$\sigma_x \approx 0.0013 \text{ of a CCD element}$$

The other noise sources can be obtained in a similar manner, after which we root-sum-square all the noise and error terms. The result, denoted by σ_T or N_T, will be about 0.006 of a CCD element. Since every pixel size is about 32.1 x 53.5 $\widehat{sec}$, it follows that the noise equivalent angle is 0.19 x 0.32 $\widehat{sec}$. The signal-to-noise-ratio can be defined many different ways. However, an appropriate criterion is given by

$$SNR = \frac{[\text{Power of the Signal}]^{1/2}}{\sigma_T} \tag{15}$$

in each direction.

Application to Mission Analysis

At this point we have examined the characteristics of the PPTS and considered the noise sources which can affect the performance of the CCD and have developed mathematical models for these sources. It remains to illustrate the application of the PPTS to a sample mission of interest.

In what follows, the sample mission will be taken to be a Jupiter/Saturn fly-by leading to a Uranus encounter. Because of the compactness of the Uranian system (see Figures 2 and 3) and the low light levels encountered in the outer regions of the solar system, a Uranus mission serves as an ideal example of the application of the PPTS. If feasibility for the Uranus application can be demonstrated, we can rest assured that PPTS will prove adequate for other outer-planet missions.

The Uranian system is unique among the planets of the solar system. Uranus is the third farthest planet from the sun at a mean distance of 19.2 AU. The most significant property of the Uranian system is that the planet axis-of-rotation and the satellites orbits are inclined approximately 90° relative to the axes of the other planets of the solar systems. The reasons are unknown. It is assumed by the scientific community that the axial tilt could have been produced by the collision of the forming planetary core with a body having approximately 7 percent of its mass. It is further assumed that satellite system formed after the tilt of the planet had occurred. Uranus has an equatorial diameter of about 50000KM

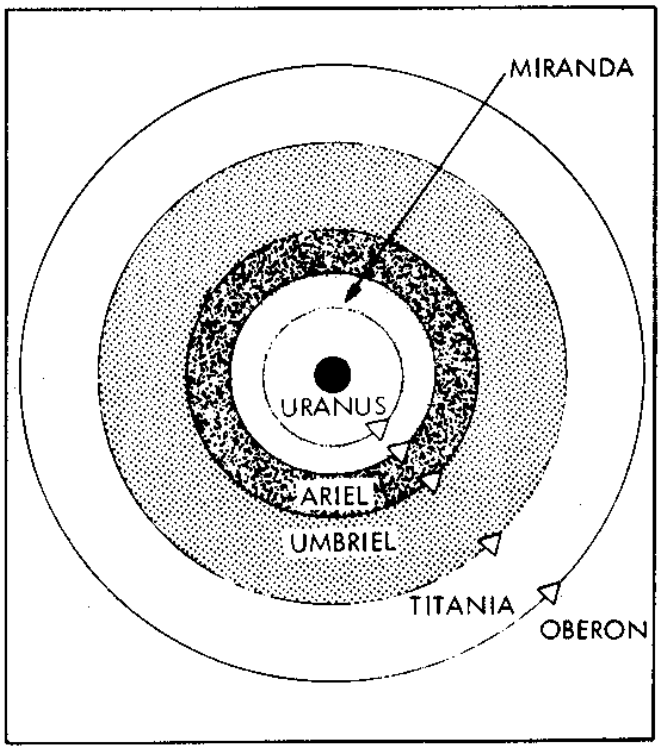

Fig. 2 — Uranus System Approach View

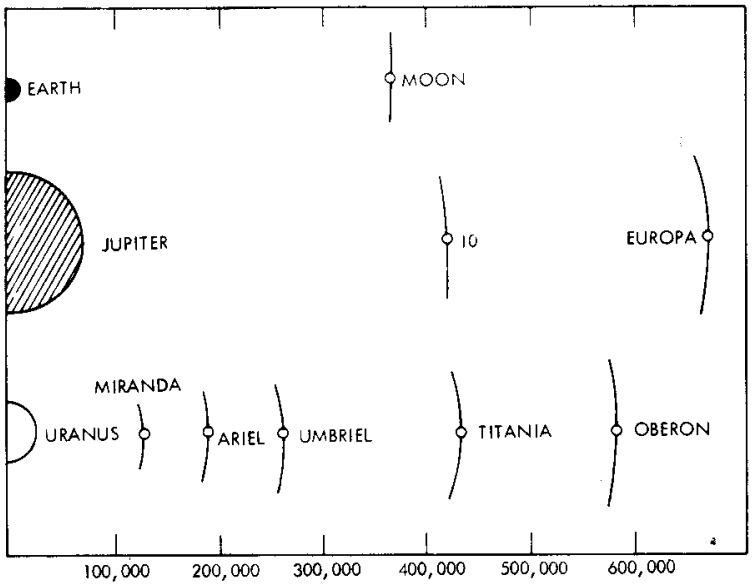

Fig. 3— Compact Uranian Satellite System

and is fifteen times more massive than earth, although its density is one-fourth that of the earth's. Based on the present knowledge about Uranus and the amazing compactness and regularity of the satellite system (Fig. 2), it is speculated that Uranus differs from Jupiter and Saturn in its chemical composition as much as it differs from terrestrial planets.

A departure from selenium-sulfus vidicon cameras used in the Mariner camera system is the availability of CCDs to provide greatly increased quantum efficiency in the near infrared (important for Uranus imaging science). The CCD sensors exhibit very low pre-amp readout noise and the dynamic range is much higher than that of the vidicons. A possible configuration to be considered for imaging science experiments would consist of three CCD cameras each with filter wheels; one with 50 mm optics, one with 200 mm optics, and one with 1500 mm optics. The 1500 and 200 mm optics would be used for trajectories of 5 RU* encounter distances, and a 1500 and 50 mm optics combination would be used less than 5 RU. A CCD with 488 x 380 pixels and the same readout rate as planned for the Voyager (48 sec per frame) takes twice as long to take a picture. For a resolution of 8 bits, the corresponding read-out rate for the CCD is every 14 s, thus a picture can be taken every 28 s. This is extremely valuable during near encounter sequences, because the CCD pictures could be obtained much faster than those from the corresponding vidicon.

It is required to permit pointing of 0.25° field-of-view (FOV) instruments with sufficient precision to locate bodies and point sources approximately the size of the instrument FOV and also point accurately at specific features on a body that are larger than the instrument FOV. The ability to have complete coverage of an area larger than the FOV of an instrument requires scanning the area. A complete mosaic is obtained by moving the scan platform in a way which allows the instrument to observe adjacent areas. To eliminate holes in the area coverage, adjacent areas are overlapped (10-50%). In obtaining a mosaic the slew from one picture to the next, and thus the taking of two pictures requires 56s. The tracker exposure time is typically 0.01 s. In some cases the science cameras exposure time could be as high as 11.5s (wide angle camera), requiring precision tracking for extended periods of time.

Mission sequencing is a function of whether we would have a Uranus orbiter or a fly-by. In either case the configuration of the outer planets is extremely important from the energy viewpoint. For example, if we want a fly-by past either Jupiter or Saturn, there are favorable launch opportunities from 1979 - 2027 where either a Jupiter/Uranus or a Saturn/ Uranus fly-by can be selected. Single launches to Uranus would have flight times on the order of 5.6 years. However, there are trajectories that may take over 7.9 years. In the case of a Uranus fly-by, there are trajectories that could allow the radius of closest approach to be as low as 1.1 RU, but the radius of approach will generally be 1.5 - 2 RU.

To estimate the approximate minimum velocity of the closest approach we shall use the simple Newtonian Formula F = Ma. The formula gives rise to $v = (GM/R)^{1/2}$, where R is the radius of closest approach in meters, $G = 6.673 \times 10^{-11}$ m^3/k_g sec^2 and $M = 10^{26}$ kg. The velocity of the closest approach will be found to be about 13 Km/s.

* Each RU is 27000Km

A most demanding requirement of the PPTS is to track features or landmarks at high velocities (400 $\frac{\text{sec}}{\text{s}}$), and to provide image motion compensation. Based on a close approach of 1.5 RU, PPTS will be able to track Uranus and its satellites (as point sources).

The five satellites of Uranus are of unknown masses and poorly known radii (ranging from 100-2000 Km). Fig. 3 demonstrates the compactness of the Uranan system as compared to the system of Earth and Jupiter.

In case of Uranus fly-by, satellite encounters will require precision arrival timing for tracking coverage. Significant science can telemetered as early as 1.5 years before Uranus encounter. The Uranus events, such as satellites closest approach, terminator crossing, feature tracking, and planet closest approach will occur nearly simultaneously. Resolutions of 1-5 Km may be possible for Uranus and its satellites.

Since the science platform is decoupled from the spacecraft, the star mapping initiation will not require more than the settling time of the closed loop control system (0.3s). For both Viking and Voyager the star mapping wait is on the order of 5 minutes due to disturbances in the spacecraft motion. The sequence prior to satellite encounters will include a full planetary mosaic three hours before the closest encounter.

Conclusion

The Planetary Pointing and Tracking System (PPTS) will provide precision scan platform articulation for a wide variety of future unmanned, planetary spacecraft. The PPTS design approach utilizing a CCD optical sensor for closed-loop control with respect to the target body, a gyro for internal stabilization, and brushless dc torque motors for smooth and continuous, platform articulation is very viable and indeed essential for high resolution planetary imaging and automated science execution. The correlation tracker is the most important tool in the PPTS. Since the probability of correct target body acquisition is a function of SNR, a detailed noise and error analysis has been performed. It has been determined that the use of on-board systems such as the CCD, are very important for image and data storage for both the far and near encounter phases. Mass data storage similar to the Mariner type missions is highly desirable for the near encounter phase as well as full frame, full resolution pictures during the far encounter phase. Both can be accomplished with CCD sensors. Due to the low intensity light levels at the outer-planets, and because vast amounts of high-quality data that has to be telemetered to earth, the use of correlation tracking becomes of great importance.

Acknowledgement

I would like to thank Drs. Michael Griffin and Robert Armstrong for reviewing the paper. The research described in this paper was carried out at the Jet Propulsion Laboratory, California Institute of Technology, under NASA Contract NAS7-100.

References

[1] P. M. Salomon and W. K. Goss, "A Microprocessor-Controlled CCD Star Tracker," AIAA 14th Aerospace Sciences Meeting, Washington, D. C. , Jan. 26-28, 1976.

[2] M. W. Johnson, "Analytical Developments and Test Results of Acquisition Probability for Terrain Correlation Devices Used in Navigation System," AIAA 10th Aerospace Sciences Meeting, San Diego, Calif. Jan. 17-19, 1972.

[3] D. F. Darbe, "Imaging Devices Using Charge-Coupled Concepts," Charged-Coupled Devices: Technology and Applications, IEEE Press, 1977.

[4] W. K. Pratt, "Laser Communication Systems." John Wiley, 1969.

[5] A. Papoulis, "Probability, Random Variables, and Stochastic Process," McGraw-Hill, 1965.

[6] R. E. Hill, JPL Internal Report 760-177 "Preliminary Design with Supporting Studies of Focal Plane Guidance Sensor Using a Charge Coupled Image Detector for Space Shuttle Infrared Telescope Facility, Final Report," May, 1977.

[7] CCD 211-244 x 190 Element Area Image Sensor Charge-Coupled Device (Fairchild Semiconductor Preliminary Data Sheet, March 1976), Charge-Coupled Devices: Technology and Applications, IEEE Press, 1977.

[8] J. R. Hyde and R. A. Wallace, "The Mariner Jupiter/Uranus, 1979 Mission," AIAA/ AGU Conference on The Exploration of the Outer Planets," St. Louis, Missouri, Sept. 17-19, 1975.

[9] J. W. Moore, "Science Planning and Mission Strategy for the 1979 Jupiter/Uranus Opportunity," The same conference as reference [8].

[10] "The Planetary Pointing and Tracking System Performance Objectives and Design Approach," JPL Internal Report 760-192, Sept. 1977.